

Verification and Mitigation of Seismic Failure in Concrete Piers under Near-field Earthquakes

Shoji Ikeda¹⁾ · Kazuhiko Hayashi²⁾ · Toshihiko Naganuma³⁾

ABSTRACT >> This paper verifies the difference of the seismic behavior and seismic damage of the neighboring two reinforced concrete piers damaged by the 1995 Hyogoken Nanbu earthquake. The two piers were almost the same size, carrying slightly different dead load, and were provided with the same reinforcement arrangement except the amount of longitudinal reinforcement at the bottom portion of the piers. The pier with more reinforcement was completely collapsed due to this near field earthquake by shear failure at the longitudinal reinforcement cut-off while the other was only damaged at the bottom by flexure even though the longitudinal reinforcement cut-off was also existed at the mid height of the pier. According to the results of the pseudo dynamic test, the seismic damage was recognized to be greatly dependent on the ground motion characteristics even though the employed ground motions had the same peak acceleration. The severe damage was observed when the test employed the seismic wave that had strong influence to the longer period range compared to the initial natural period of the pier. On the other hand, based on the similar model experiment, the defect of gas-pressure welded splice of longitudinal reinforcement was revealed to save the piers against collapse due to the so-called fail-safe mechanism contrary to the intuitive opinion of some researchers. It was concluded that the primary cause of the collapse of the pier was the extremely strong intensity and peculiar characteristics of the earthquake motion according to both the site-specific and the structure-specific effects.

Key words concrete pier, near field earthquake, cut-off, gas-pressure welded splice, fail-safe mechanism

1. INTRODUCTION

Mitigation and prevention of seismic failure of reinforced concrete piers in the highway viaduct against severe earthquakes are crucial matters to the society during and after earthquakes. Lessons from the proper verification of the actual seismic failures are essential for the mitigation of the future seismic disasters.

Urban expressway viaducts were severely damaged due to 1995 Hyogoken Nanbu earthquake and some of them were resulted in collapse⁽¹⁾. There was a case that a reinforced concrete pier was completely collapsed but its adjacent pier withstood the earthquake and had

relatively minor damage even though the two piers were almost the same size, carrying slightly different dead load, and were provided with the same reinforcement arrangement except the amount of longitudinal reinforcement at the bottom of the piers. The fact is that the pier with more reinforcement was completely collapsed due to the earthquake by shear failure at the longitudinal reinforcement cut-off while the other was slightly damaged at the bottom by flexure even though the longitudinal reinforcement cut-off was also existed. The two piers were designed in accordance with the same highway bridge design specification so that it was considered to be very important to clarify the reason why the damage of the two piers was so different. On the other hand, rupture of splices of reinforcement jointed by gas-pressure welding was seen in many piers so that some researchers have been insisting based on their intuitive opinion that the primary cause of the collapse of the pier was the rupture of gas-pressure welded splices of longitudinal reinforcement. In order to clarify the

¹⁾ Emeritus Professor, Yokohama National University, Hybrid Research Institute Inc., Japan

²⁾ Research Associate, Yokohama National University, Japan

³⁾ Senior Manager, Hanshin Expressway Company Limited, Japan
(대표저자: ikeda@hybridresearch.co.jp)

본 논문에 대한 토의를 2007년 10월 31일까지 학회로 보내 주시면 그 결과를 게재하겠습니다.

(논문접수일 : 2007. 7. 6 / 심사종료일 : 2007. 7. 24)

seismic damage described above, reversed cyclic loading tests and pseudo dynamic tests were carried out and verification of the damage and collapse mechanism of the two piers was performed.

2. OBJECTIVE OF STUDY

A concrete pier of the viaduct of Hanshin Expressway suffered to complete collapse in 1995 Hyogoken Nanbu Earthquake. The collapsed pier was seen to be extremely unusual and unseen feature as shown in Photo 1.



〈Photo 1〉 Collapsed Pier

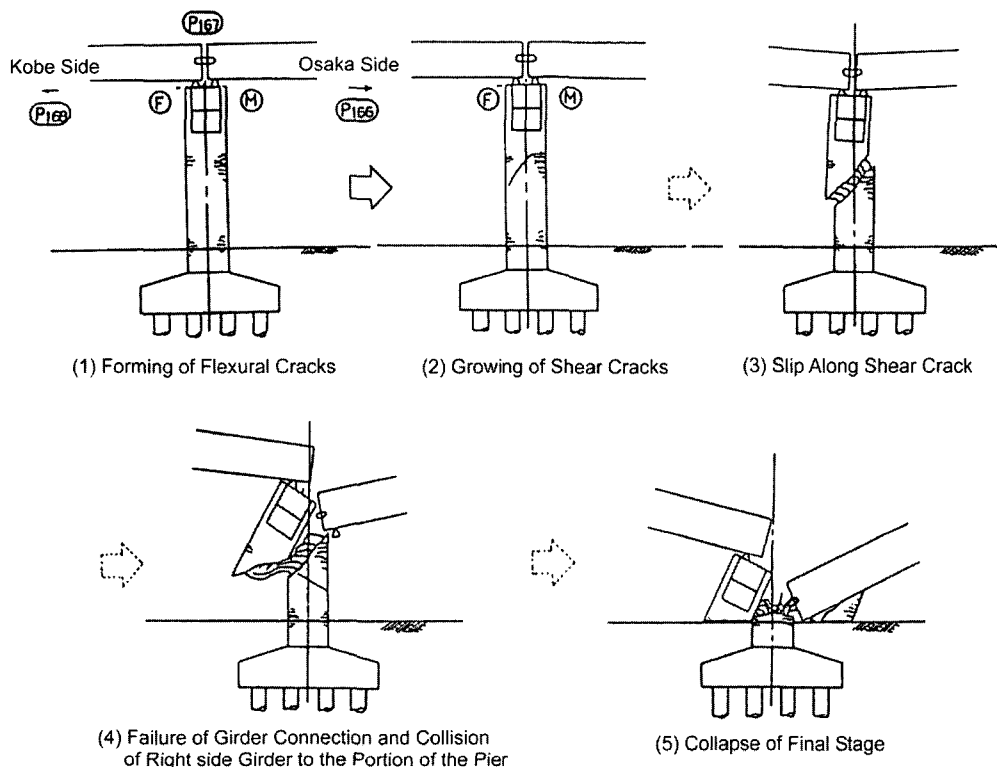
The mechanism of collapse was deliberately estimated as shown in Figure 1 in the report issued soon after the earthquake⁽²⁾. On the other hand its adjacent pier withstood without severe damage. Therefore, detailed investigation was required to find the real cause of the collapse. Structural defects such as inadequate design, corner-cutting of execution, or defect of gas-pressed welded splices of reinforcement were blamed as the primary cause of the collapse in mass media without any scientific basis. Therefore, thorough scientific investigation was necessary to verify the cause of collapse of the pier together with the reason why the adjacent pier withstood against the same earthquake.

Static reversed cyclic loading tests and Pseudo dynamic tests were expected to clarify the incident in addition to the analytical study and the review of the original design of the structures.

3. EFFECT OF EARTHQUAKE MOTION

3.1 EXPERIMENT

Two types of specimens, type A and B, that were exact 1/7-scale models of the two piers described above



〈Figure 1〉 Estimated Mechanism of Collapse of the Prototype Pier [2]

were employed to clarify the difference of the damage. Figure 2 and Table 1 show the reinforcement ratio, reinforcing bar arrangement, moment capacity, and shear capacity of the two specimens⁽³⁾.

The specimen was cantilever circular solid pier with spread footing. The diameter of the pier was 400mm and

the height from the bottom of the pier to the loading point was 1680mm. The type A specimen had a one cut-off of the longitudinal reinforcement at the mid height of the pier and the type B specimen had two cut-offs. The longitudinal reinforcement of the type A specimen was cut-off at 840mm above the bottom of the

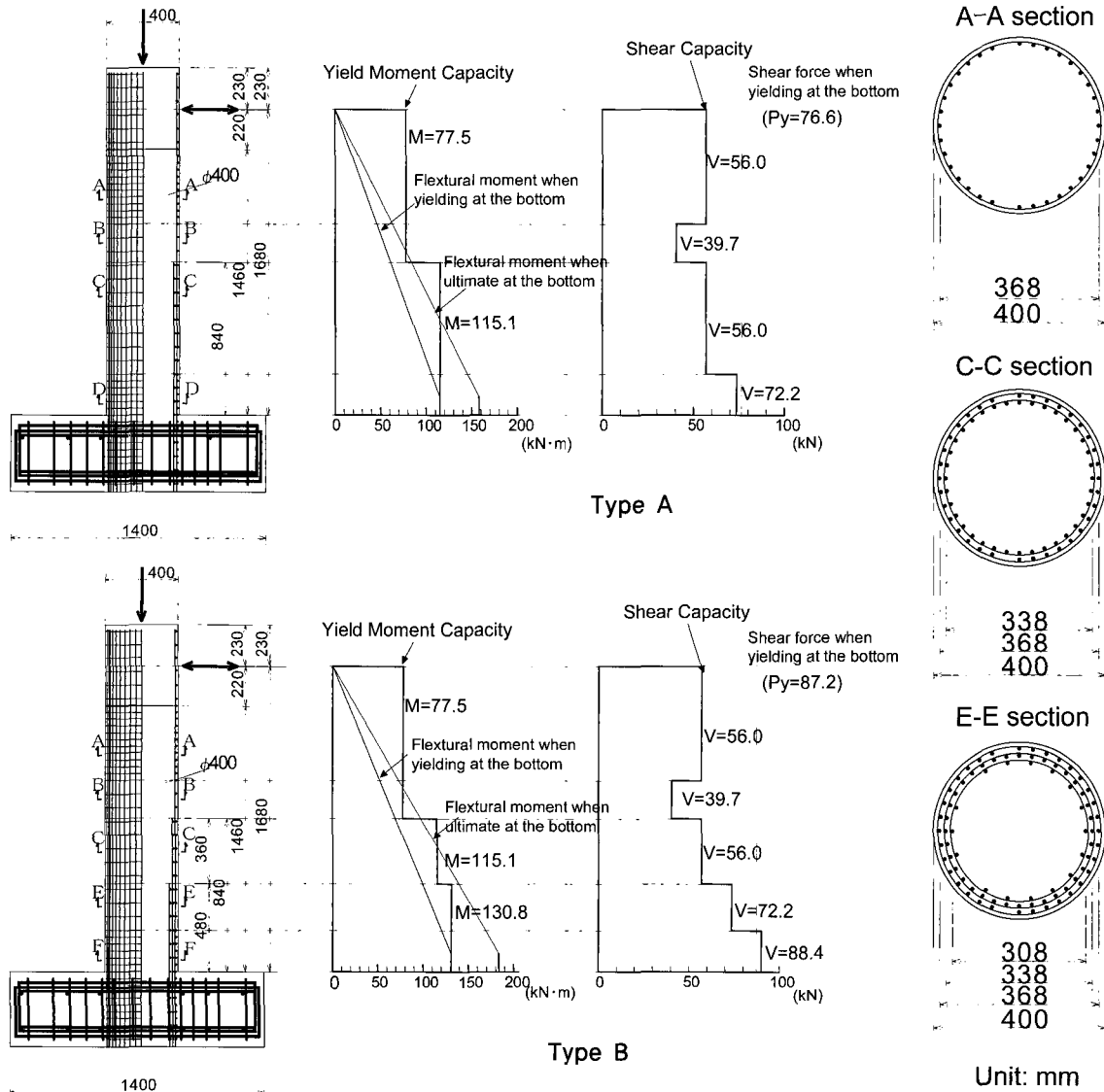


(Figure 2) Reinforcing Bar Arrangement of Specimen and Calculated Moment and Shear Capacity

(Table 1) Specimen Details

Specimen	Longitudinal Reinforcement Ratio (%)						Hoop Reinforcement Ratio (%)					
	A-A*	B-B*	C-C*	D-D*	E-E*	F-F*	A-A*	B-B*	C-C*	D-D*	E-E*	F-F*
Type A	0.91		1.81				0.0971	0.0485	0.0971	0.146		
Type B	0.91		1.81		2.27		0.0971	0.0485	0.0971		0.146	0.194
Specimen	Moment Capacity (kN·m)						Shear Capacity (kN)					
	A-A*	B-B*	C-C*	D-D*	E-E*	F-F*	A-A*	B-B*	C-C*	D-D*	E-E*	F-F*
Type A	77.5		115.1				56.0	39.7	56.0	72.2		
Type B	77.5		115.1		130.8		56.0	39.7	56.0		72.2	88.4

pier and that of the type B was cut-off at 480mm and 840mm. The important difference between the type A and type B specimen was the amount of the longitudinal reinforcement at the bottom of the pier. The weight of the superstructure that the type B supported was slightly greater than that of type A so that the amount of the longitudinal reinforcement of type B was greater than that of type A.

Hoop reinforcement was jointed by lap splice method with the development length of thirty times the diameter of the hoop reinforcement. The mechanical properties of concrete and reinforcement are shown in Table 2 and 3.

The moment capacity shown in Figure 2 was calculated by the fiber model analysis with considering material non-linearity. The yield moment is the moment when the reinforcement at the tension side at the D/4 from the bottom reaches yield where D is the diameter of the specimen. The shear capacity is calculated by 1996 JSCE design specification for concrete structures⁽⁴⁾.

In order to clarify the difference of the seismic damage, reversed cyclic loading tests and pseudo dynamic test

were carried out. Three ground motions, T. Sta. Ground Motion⁽⁵⁾, A. Ground Motion, and T. Ground Motion, which had the same peak acceleration, were employed for the pseudo dynamic tests.

3.2 STATIC REVERSED CYCLIC LOADING TEST

3.2.1 Loading method

In order to clarify the ductility characteristics of the specimens, static reversed cyclic loading tests with one cycle loading for each loading step were performed. Horizontal load was applied under the constant axial stress that was equivalent to the actual compression stress (=1.75MPa). The loading displacement of each step was 8.4mm that was calculated from 1/200 rotation angle (=Horizontal displacement / the distance between the loading point and the top of the footing).

3.2.2 Test result

The test result is summarized in Table 4. Photo 2 shows the tested specimens subjected to reversed cyclic loading. The yield displacement was defined as the mean

(Table 2) Mechanical Properties of Concrete

Experiment Case*1	Specimen	Loading Method	Compression Strength (MPa)	Tensile Strength (MPa)	Young's Modulus (GPa)
A-ST	Type A	Static Reversed Cyclic Loading	34.3	2.5	27.5
B-ST	Type B		34.3	2.5	27.5
B-PD-T	Type B	Pseudo Dynamic	32.5	2.4	24.2
A-PD-A	Type A		34.8	2.4	24.8
B-PD-A	Type B		32.3	2.6	24.1
A-PD-T.Sta	Type A		34.8	2.3	24.8
B-PD-T.Sta	Type B		32.3	2.5	25.5

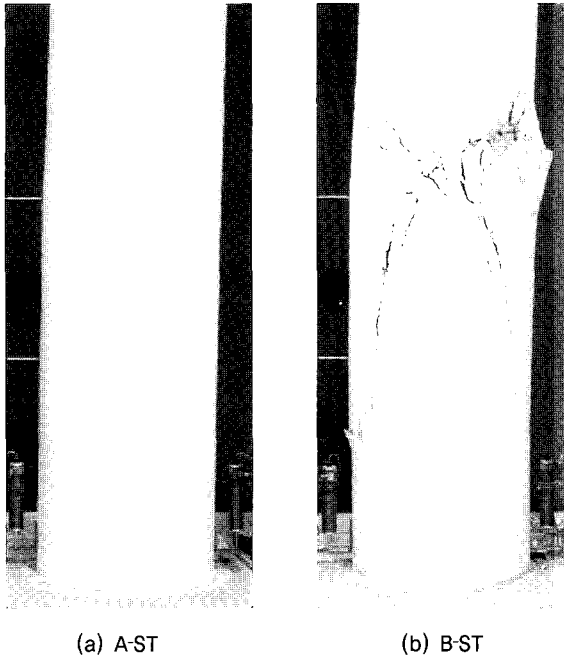
*1: ST: Static reversed cyclic loading test, PD: Pseudo dynamic test, T: Generated ground motion at the site, A: Observed ground motion at Amagasaki viaduct, T.Sta: Observed ground motion at JR Takaroti station

(Table 3) Mechanical Properties of Reinforcement

Reinforcement	Category	Yield Strength (MPa)	Tensile Strength (MPa)	Young's Modulus (GPa)	Application
D3	SD295	326	390	203	Hoop Bars
D6	SD345	395	623	174	Longitudinal Bars

(Table 4) Experimental Result of Static Reversed Cyclic Loading Test

Specimen	Yield Displacement δ_y (mm)	Ultimate Capacity P_{max} (kN)	Ultimate Displacement δ_u (mm)	Ductility δ_u/δ_y
A-ST	8.5	106	58	7
B-ST	9.4	111	39	4



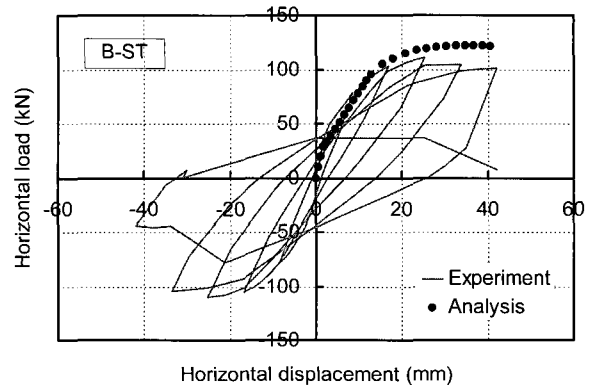
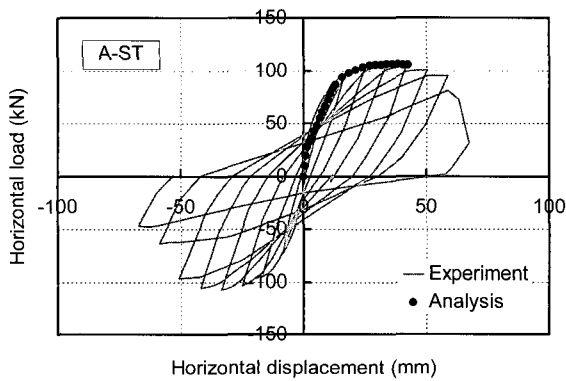
〈Photo 2〉 Damage Observed in Static Cyclic Loading Test (at -5/200 rad. loading)

of the positive and negative displacement when the computed yield force was applied. Figure 3 shows the load-displacement relation of each specimen. Computed ductility curve obtained by push over analysis using fiber model is also shown in the same figure. The computed ductility curve includes not only flexural displacement but also shear displacement. The ultimate state of the computed ductility curve was determined where the compression strain of the compression fiber reached to 0.35%. The computed ductility curve almost enveloped the experimental cyclic force-displacement curve in the case of type A. However, the computed and experimental curves were slightly different after yield in the case of

type B because shear damage was progressed and the type B specimen failed at the mid height of the pier before the bottom of the pier reached the flexural ultimate state.

The ultimate displacement was $7\delta_y$ (δ_y : yield displacement measured by the experiment) in the case of type A and $4\delta_y$ in the case of type B. In this paper, the ultimate displacement was defined as the displacement where the horizontal restoring force was decreased to 80% of the peak restoring force. The flexural strength of the type B specimen was greater than that of the type A specimen, therefore, the stiffness of the bottom part of the type B specimen became large. This resulted in the concentration of deformation at the longitudinal bar cut-off and in reduction of ductility capacity. On the other hand, the flexural strength of the type A specimen was less than that of the type B specimen. This resulted in less acted shear force and the less concentration of rotation at the longitudinal bar cut-off. Consequently, more ductile behavior was observed.

The results of the static cyclic loading test can be summarized as follows: The type A and type B specimen satisfy the seismic demand at the time of the construction of the prototype structures where the strength of the type B specimen was greater than that of the type A specimen due to the design requirement. However, this greater flexural strength required more shear strength and this resulted in concentration of deformation and reduction of ductility capacity at the longitudinal bar cut-off where was the smallest shear capacity in the specimen. Contrarily, less flexural strength resulted in less shear capacity



〈Figure 3〉 Result of Cyclic Load-Displacement Relation

demand and less damage at the longitudinal bar cut-off region in the case of the type A specimen.

3.3 PSEUDO DYNAMIC LOADING TEST

3.3.1 Experiment setup

Three ground motions, T. Sta. Ground motion, A. Ground Motion, and T. Ground Motion, which had the same peak acceleration, 600 gals, were employed for the tests. T. Sta. Ground Motion and A. Ground Motion are measured ground motions observed at JR Takatori station and the Amagasaki viaduct at the 1995 Hyogoken Nanbu earthquake respectively, which contain relatively strong low frequency components. The T. Ground Motion is an artificially generated ground motion which contains relatively strong high frequency components. The intensity of each wave was scaled to 600 gals at the peak acceleration because the peak acceleration at the construction site of the prototype piers was estimated over 500 gals and biaxial loading effect was also considered. Figure 4 shows the acceleration response spectrum of each employed seismic wave. In the longer period region over 1.0 sec, there is the difference among the three waves.

Initial stiffness was determined using the result of the static cyclic loading test, i.e., secant stiffness of origin to

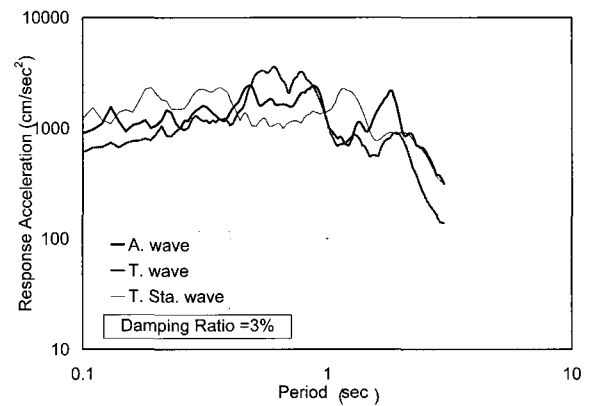
the cracking point, was 21.0 kN/mm for the initial stiffness.

Initial natural period was set to 0.55 sec for the type A specimen and 0.59 sec for the type B specimen according to the values of the prototype structures. The virtual mass was 157.9 ton for type A and 181.7 ton for type B.

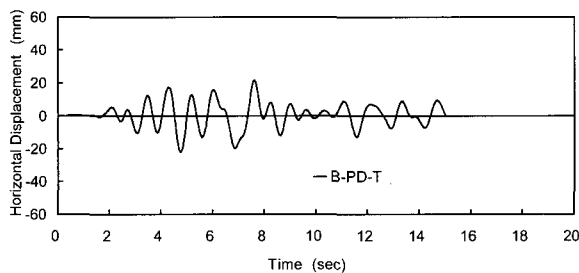
Initial damping ratio was set to 3% and decreased to 0% where the secant stiffness decreased to 25% of initial stiffness⁽³⁾.

3.3.2 Test result

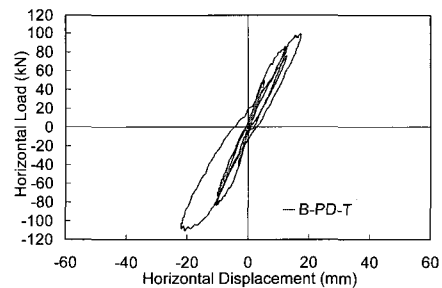
Figures 5, 6, and 7 show the displacement time history and the restoring force and response displacement



<Figure 4> Acceleration Response Spectrum

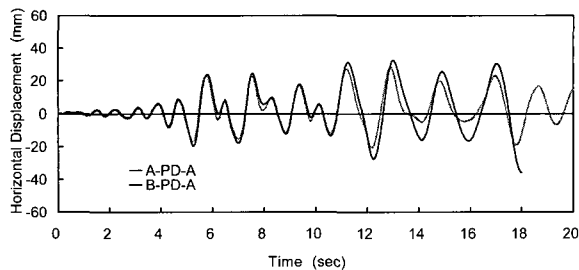


(a) Time history of response displacement

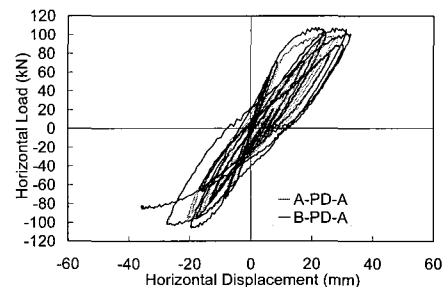


(b) Restoring force and response displacement

<Figure 5> Result of Pseudo Dynamic Test (B-PD-T)

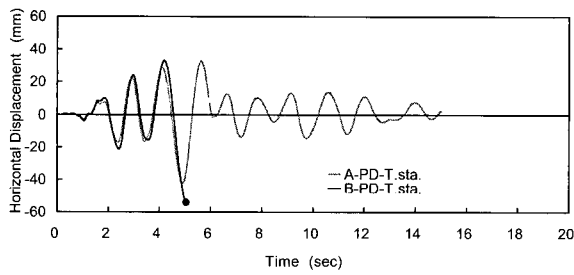


(a) Time history of response displacement

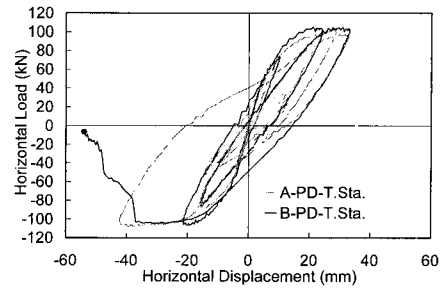


(b) Restoring force and response displacement

<Figure 6> Result of Pseudo Dynamic Test (A-PD-A, B-PD-A)

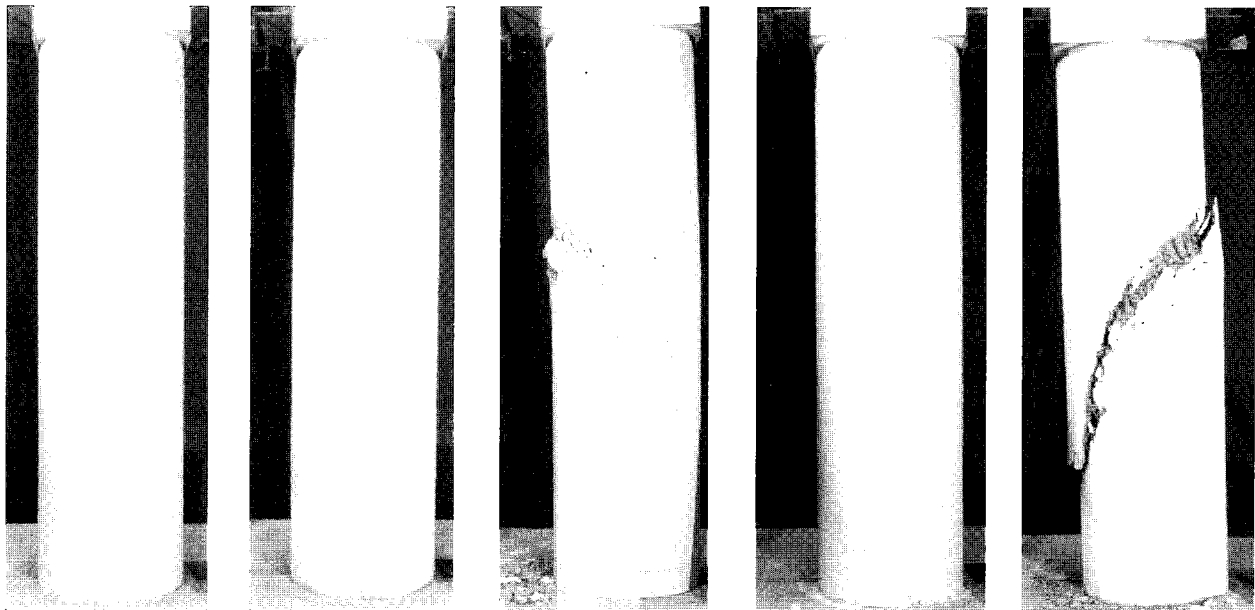


(a) Time history of response displacement



(b) Restoring force and response displacement

(Figure 7) Result of Pseudo Dynamic Test (A-PD-T.Sta., B-PD-T.Sta.)



(a) B-PD-T

(b) A-PD-A

(c) B-PD-A

(d) A-PD-T. Sta.

(e) B-PD-T. Sta.

(Photo 3) Damage of Each Specimen Subjected to Pseudo Dynamic Test

relation.

Even though the peak acceleration of the applied seismic waves was scaled to 600 gals, the response characteristics of each wave were completely different because of the characteristics of the frequency component. The response displacements subjected to A. wave and T. Sta. wave were relatively large. The natural period of each specimen was 0.55 and 0.59 sec so that the degraded natural period when the damage was progressed might exceed 1.0 sec. As A. wave and T. Sta. wave had greater response acceleration over 1.0 sec range, these phenomena were the possible reason of the larger response displacement.

According to Photo 3, the big difference of the damage was observed where T. Sta. wave was applied. The type B specimen suffered sudden slip that resulted in collapse.

On the other hand, the type A specimen suffered minor shear crack at the longitudinal bar cut-off and no strength reduction was observed.

The difference of the ductility characteristics of the neighboring two piers resulted in the difference of the seismic damage even though subjected to the same earthquake ground motion. This means that it is not strange that one pier collapsed and the adjacent pier withstood the earthquake.

3.4 RESPONSE ANALYSIS

The response of each specimen was analyzed by the SDOF non-linear model. Figure 8 shows the non-linear restoring force characteristics used for the model. The model can express the softening stiffness when unloading. The feature of this restoring force model is to express the

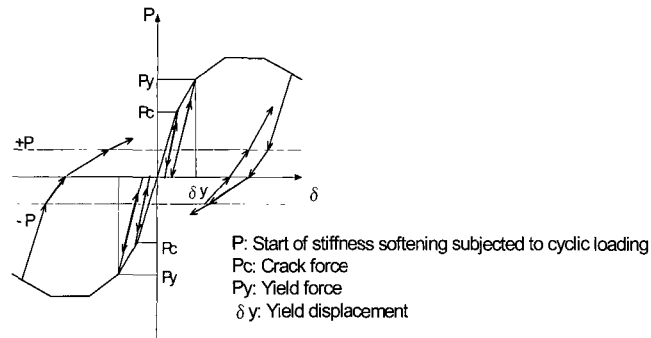
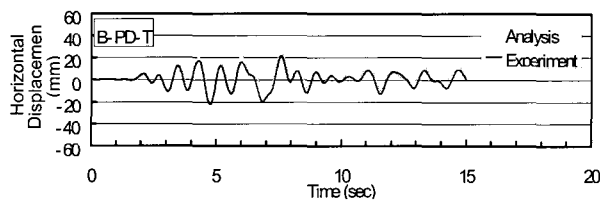
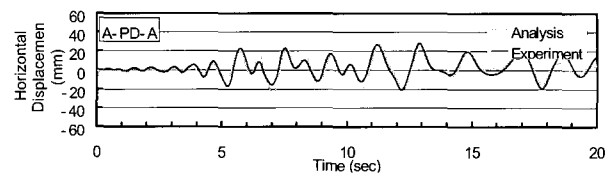


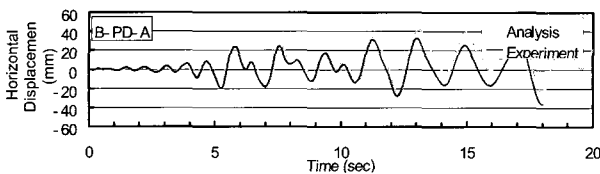
(Figure 8) Restoring Force Model



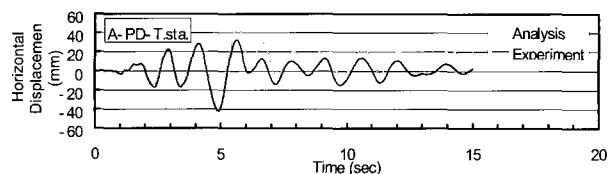
(a) Response displacement (B-PD-T)



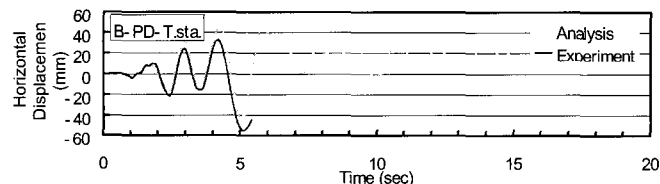
(b) Response displacement (A-PD-A)



(c) Response displacement (B-PD-A)



(d) Response displacement (A-PD-T,Sta.)



(e) Response displacement (B-PD-T,Sta.)

(Figure 9) Comparison of Analytical and Experimental Results

skeleton curve by using multi lines and to make any type of skeleton curve obtained by static cyclic loading test.

Figure 9 shows the comparison of the response displacement time history obtained by experiment and analysis. According to Figure 9, the analytical result can simulate the experimental result. Therefore, the restoring force model was ascertained to simulate the response of concrete piers subjected to severe earthquakes.

4. DEFECT OF GAS-PRESSURE WELDED SPLICES

The failure of gas-pressure welded splices in the reinforced concrete pier was widely observed in the

damaged structures after the earthquake. Eventually some inexperienced researchers and engineers based on their intuitive opinion have been insisting that the primary cause of collapse of the pier was the rupture of gas-pressure welded splices of longitudinal reinforcement since welded portions did not melt apparently. It should be noted that the principle of gas-pressure welding is the diffusion of atoms at the contact planes so that steel does not melt at the time of welding process. Therefore, connecting planes are sometimes separated in case of the failure at the splices even if tensile stress in the reinforcement reaches the yield point. Accordingly it is difficult to evaluate the quality of gas-pressure welded

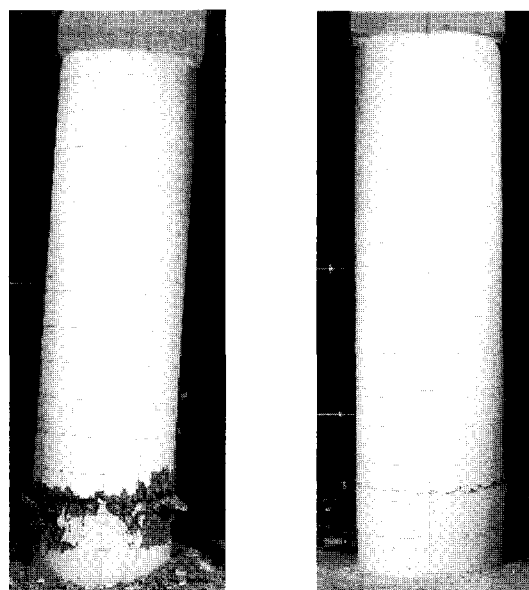
splices by only apparent observation. Obviously this kind of failure should be avoided and sufficient inspection must be necessary to obtain gas-pressure welded splices in good quality.

Nevertheless, the collapse of the pier should not be attributed to the rupture of gas-pressure welded splice without scientific investigation. Hence, static reversed cyclic loading test and pseudo dynamic test were performed to clarify the relationship between the collapse of the pier and the rupture of the splices⁽⁶⁾.

The size and shape of the model specimens were identical to the previous experiment. The assumed defect of the gas-pressure welding was designated such that three fourths of the cross section of outer longitudinal reinforcement were removed by a cutting machine. Since ratio of area of outer, middle, and inner reinforcement are 0.4, 0.4, and 0.2 as shown in Figure 2 (Type B) respectively, the ratio of outer one reduced to $0.4 \times 1/4 = 0.1$. Therefore, total of reinforcement became 0.7 instead of 1.0. Furthermore, after the cut bars were broken, in other words, defective splices were broken, total ratio became 0.6.

According to the prototype pier, the location of the cut section in the specimen was 230mm above the surface of the footing. It is noted that all the outer reinforcement of the prototype pier of the Type B specimen was gas-pressure welded at the same height.

In the pseudo dynamic test T. Sta. Ground Motion was applied with peak acceleration of 600 gals as same as the previous experiment. Photo 4 shows the experimental results of static reversed cyclic loading test and pseudo dynamic test in which predominant flexural crack appears at the location of the cross section of virtual defective splices and no diagonal tension crack can be seen. The specimens showed ductile flexural manner although the maximum load was less than that of the specimen without cut bars. The experimental results clearly show that the pier does not collapse if the defect of the splices exists. This means that the defect of the gas-pressure welded splices is not only innocent to the collapse but also the defect can save the pier against the earthquake by fail-safe mechanism. This experimental finding is coincident with the actual concrete piers



(a) Reversed Cyclic Loading Test (b) Pseudo Dynamic Test

〈Photo 4〉 Tested Specimens Referring to the Defect of Gas-Pressure Welding

standing after the earthquake which had damage due to the rupture of the gas-pressure welded splices.

5. DISCUSSION AND VERIFICATION

5.1 Verification

According to the test results of reversed cyclic loading, less ductile behavior was observed for the pier with more longitudinal reinforcement, so that more reinforcement resulted in less ductility due to the corresponding increase of shear force. In addition the cut-off of longitudinal reinforcement in the pier reduced the integrity against the horizontal disturbances. According to the result of pseudo dynamic test, the degree of seismic damage was clearly recognized to be greatly dependent on the ground motion characteristics in spite of the same peak acceleration.

The collapse was observed in the specimen having larger reinforcement when the test employed the seismic wave which had strong influence to the longer period range compared to the initial natural period of the pier. The specimen with less longitudinal reinforcement withstood the same seismic ground motion without significant damage by shear.

In the above mentioned experiments, it was clearly realized that one pier collapsed while the adjacent pier

survived. Therefore, the cause of the collapse was not the structural defect such as inadequate design, corner cutting of execution, or defect of gas-pressure welding. Furthermore, it was clarified that the defect of gas-pressure welded splices could rather save the pier against collapse due to the so-called fail-safe mechanism, contrary to the intuitive opinion of some researchers even if the defect of the splices existed.

It can be said that the primary cause of the collapse of the pier was extremely strong intensity and peculiar characteristics of the earthquake ground motion in the condition that the pier was correctly constructed with the allowable stress design method. To learn from this disaster, comprehensive discussions based on the results of this study should be necessary together with reviewing the actual failures of the structures under the near field earthquake. The estimated collapse mechanism depicted in the committee report issued soon after the earthquake as shown in Figure 1 was proven to be correct by the pseudo dynamic test. This proper estimation should be highly appreciated.

There have been a lot of controversial disputes and discussions after the earthquake relating to the responsibility of the seismic collapse. However, the collapse is a mechanical phenomenon of the structure in which rupture, crash and segregation of materials could be seen together with minor imperfect construction. Generally speaking, these fractures are the result of the collapse and not the cause of the collapse. Mass media and hasty

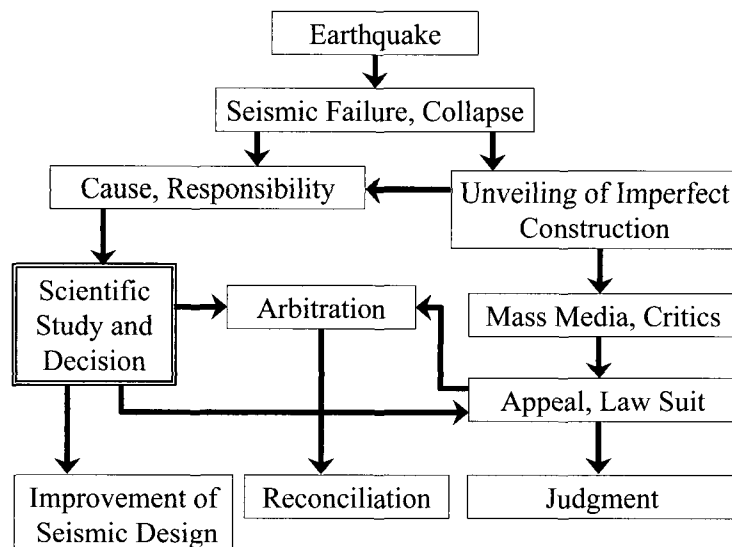
critics happen to insist wrong comments contrary to the scientific approach. Fig.10 shows that the flow of events after an earthquake where cause and responsibility are separated from the apparent failure phenomena. A proper decision based on the scientific study is obviously necessary to the improvement of seismic design and the proper judgment in the law suit. Considering the importance of the logical framework, the flow of events after an earthquake as shown in fig.10 should be useful.

5.2 Plane Fault Model

In addition to the above mentioned experiment, authors have continued to study by using the seismic waves obtained from plane fault models. Seven similar specimens were used for the pseudo dynamic test based on the plane fault models. As the result of the experiment, It was clarified that the seismic wave of the plane fault model could perform fairly good seismic disturbance including site specific effects. However, the specimen which was similar to type A failed significantly contrary to the previous test or actual behavior of the piers. Therefore, within this experiment, the actual seismic wave of JR Takatori would be more realistic compared to the one obtained from the present plane fault models.

5.3 Vertical Prestressing

Vertical prestressing in the reinforced concrete pier has been recognized quite effective against severe earthquake motions from the extensive study in Japan⁽⁷⁻¹⁰⁾.



〈Figure 10〉 Flow of Events after Earthquake

The vertical prestressing technology can mitigate seismic failure and deformations according to the structure-specific effects through performance-creative design concept.

6. CONCLUSIONS

- (1) The difference of the damage of the two adjacent piers that were almost the same size, carrying slightly different dead load, and were provided with the same reinforcement arrangement except the amount of longitudinal reinforcement at the bottom of the piers was clarified by performing static cyclic loading tests and pseudo dynamic tests. According to the experiments, the reason of the difference of the damage of the two piers attributed to the difference of the flexural capacity and eventually the difference of the shear forces induced. The pier that had slightly stronger flexural capacity and had more demand of shear capacity resulted in suffering completely shear failure and the pier that had less flexural capacity and had less demand of shear capacity resulted in suffering ductile flexural damage with minor shear crack.
- (2) It was clearly realized by the pseudo dynamic test that one pier collapsed while the adjacent pier survived. It was verified that the cause of the collapse was not the apparent structural defect, but the extremely strong intensity and peculiar characteristics of the near-field earthquake motion according to both the site-specific and the structure-specific effects while the pier was correctly constructed with the allowable stress design method.
- (3) It was revealed that the defect of gas-pressure welded splices could rather save the pier against collapse due to the so-called fail-safe mechanism.
- (4) In order to clarify the logical framework, a flow of events after an earthquake was shown for the verification of seismic failures.
- (5) Seismic waves obtained from plane fault models were examined compared with the actual observed seismic waves. It was found that the actual observed wave gave more realistic failure behavior in the pseudo dynamic test.

- (6) Combination of the site-specific and structure-specific effects can be the most crucial concept of the seismic design for the prevention and the mitigation of the seismic failures. Vertical prestressing technology would be the one of the rational way for seismic mitigation in performance-creative design.

ACKNOWLEDGEMENT

The authors greatly appreciate Prof. Tastuya Tsubaki, Dr. Yukio Adachi and Dr. Takahiro Yamaguchi for their contribution to the research project.

REFERENCE

1. Adachi, Y., Ishizaki, H., Ikehata, S., Ikeda, S., "Verification of the Failure of Reinforced Concrete Piers Under the Near-Field Earthquake," *Proceeding of the 1st fib Congress 2002*, Vol. 5, Session 6, Oct. 2002, pp. 389-396
2. "Committee in the Ministry of Construction," Report on the Damage of Highway Structures by 1995 Hyogoken Nanbu Earthquake (in Japanese).
3. Ikehata, S., Adachi, Y., Yamaguchi, T., Ikeda S., "Study on Seismic Behavior of Reinforced Concrete Piers by Pseudo-Dynamic Test," *Proceedings of the Japan Concrete Institute*, Vol. 23, No. 3, Jun. 2001, pp. 1255-1260 (In Japanese).
4. Japan Society of Civil Engineers, JSCE Design Specification for Concrete Structures (Structural Design Part), Mar. 1996 (In Japanese).
5. Railway Technical Research Institute: 1995 Hyogoken Nanbu Earthquake -Strong Motion Data-, *JR Strong Motion Data File*, No. 23d, Mar. 1996 (In Japanese).
6. Fujiwara, T., Hayashi, K., Adachi, Y., Ikeda, S., "Earthquake Response of RC Bridge Piers Having a Defect at the Splice of Reinforcement," *Proceedings of the Japan Concrete Institute*, Vol. 25, No. 2, Jun. 2003, pp. 1381-1386 (In Japanese).
7. Ikeda, S., "Seismic behavior of reinforced concrete columns and improvement by vertical prestressing," *Proceeding of the 13th FIP Congress*, Amsterdam, May 1998, pp. 879-884
8. Ikeda, S., Mori, T., Yoshioka, T., "Study on the seismic behavior of prestressed concrete piers," *Journal of Prestressed Concrete*, Japan, Vol. 40, No. 5, Sept. 1998, pp. 40-47 (In Japanese).
9. Dong kyu Park, Yamaguchi, T., Ikeda, S., "Fundamental study of the Seismic Properties and Seismic Design of Prestressed Concrete Piers Considering Prestress Levels," *Journal of Prestressed Concrete*, Japan, Vol. 43, No. 2, March 2001, pp. 141-148 (In Japanese).
10. Ikeda, S., Hayashi, K., "Study of Arrangement of PC Tendons in Prestressed Concrete Piers," *Proceedings of The 14th Symposium on Development in Prestressed Concrete*, Niigata City, Japan, Nov. 2005, pp. 129-134 (In Japanese).